

Modeling of the Yield Strength Evolution in Al-Mg-Si Alloys

Peter Lang¹, Ahmad Falahati², Erwin Povoden-Karadeniz¹, Mohammad Reza Ahmadi²,
Piotr Warczuk² and Ernst Kozeschnik^{1,2}

¹Christian Doppler Laboratory "Early Stages of Precipitation", Favoritenstraße 9-11, 1040 Vienna, Austria.

²Vienna University of Technology, Institute of Materials Science and Technology, Favoritenstraße 9-11,
1040 Vienna, Austria

With the thermo-kinetic software MatCalc, simulations of the evolution of precipitates in the course of thermo-mechanical treatment of heat-treatable Al-Mg-Si alloys are performed. Based on the calculated size distributions for the different stable and metastable precipitates, the evolution of the yield strength with time during different thermal processing routes is evaluated. The strengthening model used takes into account the contributions of the intrinsic yield strength of the aluminium matrix, solid solution hardening and precipitation hardening. For precipitation hardening, the coupling effect of multiple precipitates and the shape of the precipitates are considered as well as the mechanism change from particle cutting and to Orowan looping. The model is applied to isothermal age-hardening of Al-Mg-Si alloys. The comparison between the yield strength predicted by the simulations and experiment shows good agreement.

Keywords: *Aluminium alloys, precipitation kinetics, precipitation strengthening, yield strength*

1. Introduction

With increasing computational power and using a suitable thermo-kinetic software such as MatCalc [1], it is possible to simulate the evolution of precipitation sequences in any arbitrary heat treatment, provided the required thermodynamic and mobility databases are available. Till now the main drawback had been the unavailability of a suitable thermodynamic database, which includes also the metastable phases observed in 6xxx alloys. This task has been carried out recently, where the thermodynamic data has been assessed and tested satisfactorily [2, 3].

In the presented paper, two types of approaches to calculate the yield strength evolution are utilized and validated by comparison with experimental data. The first approach is a simplified algorithm (in the following designated as Approach I) as presented in Refs. [4, 5]. This approach considers the accumulative effect of solid solution hardening and precipitation hardening due to shearing and bypassing of particles by dislocations. Input values are mean radii and volume fraction of precipitates, which have been calculated in kinetic simulations carried out with MatCalc [1].

The second approach (in the following designated Approach II) is a more sophisticated version and considers not only the solute strengthening effect, but also chemical hardening, the coherency strain effect and the modulus mismatch effect in competition with the classical Orowan mechanism for each phase. The chemical hardening effect includes anti-phase boundary effects, the stacking-fault energy (SFE) and interfacial energy effects. This approach has been already implemented in the software MatCalc and has been used for simulation of the yield strength evolution in Cu-precipitation strengthened ferritic steel [6].

The calculated yield strength with both approaches is verified against experimental results and discussed subsequently.

2. Mathematical modelling

In aluminium alloys, a number of different strengthening mechanisms are operative, which all contribute to the overall yield strength. The most important contributions to age hardening of

aluminium alloys are precipitation strengthening σ_p due to shearing and bypassing of particles by dislocations and solid solution hardening σ_{ss} [4, 5].

2.1 Approach I (simplified model)

2.1.1 Precipitation hardening

In real systems some of the particles N_i will act as weak (shearable) and the rest as strong (non-shearable) obstacles. The mean obstacle strength F_{mean} can be conveniently written as [4]

$$F_{mean} = \frac{\sum N_i * F_i}{\sum N_i} \quad (1)$$

where N_i is the number density of particles, which belong either to the weak or to the strong population. F_i is the corresponding obstacle strength.

The parameter $F_{mean,weak}$ is proportional to the particle radius r_i , as long as r_i is smaller than the critical radius for shearing r_c [4, 5]:

$$F_{mean,weak} = 2\beta Gb^2 \frac{r_i}{r_c} \quad (2)$$

G is the shear modulus of the aluminium matrix, b is the magnitude of the Burgers vector and β is a constant, usually taken as 0.36 [4].

For non-shearable (strong) particles, where the radius is bigger than the critical radius $r_i > r_c$, the obstacle strength $F_{mean,strong}$ will be independent of r_i and therefore constant [4, 5]:

$$F_{mean,strong} = 2\beta Gb^2 \quad (3)$$

The various parameters of equations (2) and (3) can be rewritten in the parameter k_{ppt} [4, 5] with

$$k_{ppt} = 2\beta GbM \sqrt{\frac{3}{2\pi}} \quad (4)$$

In the present model for approach I, the ratio for precipitation strengthening for small (shearable) particles ($r_{m_s,phase}$ = mean radius of particles smaller than critical radius) is described as

$$\sigma_{s,phase} = k_{ppt} * \sqrt{f_{phase}} * \sqrt{r_{m_s,phase}} * -1.5\sqrt{r_c} \quad (5)$$

For the large (non-shearable) particles of each phase ($r_{m_b,phase}$), the equation for usage in MatCalc reads

$$\sigma_{b,phase} = k_{ppt} * \sqrt{f_{phase}} * \sqrt{r_{m_b,phase} + 1 * 10^{-12}} \quad (6)$$

The precipitation strengthening formula used in the actual model for each phase, $\sigma_{p,phase}$ can be written as

$$\sigma_{p,phase} = \sigma_{s,phase} * \frac{np_{small,phase}}{N_{prec,phase}} + \sigma_{b,phase} * \frac{np_{big,phase}}{N_{prec,phase}} \quad (7)$$

where $np_{small,phase}$ is the number of precipitates of one phase smaller than some critical coherency radius, $np_{big,phase}$ is the number of precipitates larger than a critical coherency radius and $N_{prec,phase}$ is the total number of precipitates of each phase.

The overall macroscopic precipitation hardening influenced by all considered phases is expressed as

$$\sigma_p = \sum_i^n \sigma_{p,phase_i} \quad (8)$$

2.1.2 Solid solution hardening

The solution of the elements Mg and Si in the Al matrix gives rise to the solid solution strengthening effect. The individual terms of the strengthening contribution can be superimposed and the total solution strengthening σ_{ss} can be represented by following term [4, 5]

$$\sigma_{ss} = \sum_i^n k_i * c_i^{\frac{2}{3}} \quad (9)$$

The parameters k_i for the alloying elements are defined in Table 4, c_i is the weight fraction of the element in the matrix.

2.1.3 Overall macroscopic yield strength

The expression for the lower macroscopic yield strength LYS becomes

$$LYS = \sigma_i + \sigma_{ss} + \sigma_p \quad (10)$$

In Eq. 10, σ_i is taken equal to the intrinsic yield strength of pure aluminium ($\sigma_i = 28$ MPa) [7].

2.2 Approach II (complex model)

2.2.1 Chemical strengthening

In chemical strengthening, the increase in strength occurs due to the production of new particle – matrix interface after a precipitate is sheared by a dislocation. This effect can be represented by the following term

$$\sigma_{chem} = \frac{2M}{b\lambda T^{1/2}} (\gamma b)^{3/2} \quad \text{with} \quad \gamma = \frac{2\sigma_i}{b} \quad (11)$$

where M is the Taylor factor, T is the line tension of the dislocation, λ is the mean particle spacing in the slip plane, b is the Burgers vector, N is the number and r is the mean radius of the precipitates of each phase.

2.2.2 Misfit strengthening

Due to coherency of the early precipitates with the Al matrix and volumetric misfit strains, an elastic stress field exists in the matrix around the precipitates [6] giving rise to coherency strengthening with

$$\sigma_{coh} = 8,4MG|\varepsilon|^{1/2} \left(\frac{N}{b}\right)^{\frac{1}{2}} r^2 \quad (12)$$

In the formula, G is the shear modulus, ε is the lattice mismatch, N is the corresponding number density and r represents the mean particle radius.

2.2.3 Modulus strengthening effect

This strengthening contribution occurs due to the differences of the elastic moduli of precipitate and matrix. We have assumed that the elastic moduli of the metastable phase were similar (=120 GPa) as for elastic modulus of the stable Mg₂Si (β phase), as reported with 113.5 GPa [8].

$$\sigma_{\text{mod}} = M \frac{Gb}{\lambda} \left[1 - \left(\frac{U_1}{U_2} \right)^2 \right]^{\frac{3}{4}} \quad \text{with} \quad \frac{U_1}{U_2} = \frac{U_1^\infty \log \frac{r}{r_i}}{U_2^\infty \log \frac{r_0}{r_i}} + \frac{\log \frac{r_0}{r}}{\log \frac{r_0}{r_i}}. \quad (13)$$

U_1 and U_2 are the line energies of the dislocation in the precipitate and in the matrix. Term r_i is the inner cut-off radius of the dislocations stress field ($= 2.5b$) and r_0 is the outer cut-off radius equal to 1000 r_i . This ratio corresponds to the ratio of the products of shear modulus and Burgers vector squared [6]

2.2.4 Antiphase boundary effect

The penetration of a dislocation through a particle is accompanied by the formation of an antiphase boundary (APB). This effect can be described with [9]

$$\Delta\sigma_{APB} = 0.81M \frac{\gamma_{apb}}{2b} \left(\frac{3\pi f}{8} \right)^{\frac{1}{2}}. \quad (14)$$

The volume fraction of precipitates is given by the term f and γ_{apb} is an average value of the APB energy in the precipitate.

2.2.5 Orowan mechanism

The precipitate-dislocation interaction changes from shearing to bypassing of hard particles by looping. The corresponding stress is [6]

$$\sigma_{Orowan} = \frac{C^* GbM}{\pi\lambda\sqrt{1-\mathcal{G}}} \ln\left(\frac{2r}{b}\right) \quad \text{with} \quad \lambda = \left[\left(\frac{3\pi}{4f} \right)^{\frac{1}{2}} - 1.64 \right] r. \quad (15)$$

Where C is a constant close to 0.4 and \mathcal{G} is the Poisson ratio.

To calculate the overall precipitation strengthening effect (σ_p), the different mechanisms (2.2.1 – 2.2.4 for cutting and 2.2.5 for looping) are superimposed as

$$\sigma_p^\alpha = n_{\text{shear}}^2 \sigma_{P,\text{shear}}^\alpha + n_{\text{loop}}^2 \sigma_{P,\text{loop}}^\alpha \quad (16)$$

where n_{shear} and n_{loop} are the corresponding density fractions and σ the strengthening contributions with α being 1.

Finally, the lower yield strength (LYS) evolution can be calculated by adding the strengthening effects linearly as given in Eq. 10.

$$LYS = \sigma_i + \sigma_{ss} + \sigma_p \quad (17)$$

3. Experimental

The chemical composition of the 6016 alloy used for the experiments is given in Table 1.

The alloy was solution heat treated at 550°C for 1h, water quenched to room temperature (RT) at 25°C, stored at RT for 6 days and finally aged at 185°C for 8h and tested.

Sample preparation and tensile tests were carried out according to the standard EN 10002-1.

Table 1. Chemical composition of experimental aluminium alloys (in wt.%)

Alloy	Si	Mg	Cu	Mn	Fe
I	1.07	0.34	0.07	0.07	0.18

4. Results

For the numerical simulations in MatCalc [1], the input data are summarized in Tables 2 and 3. The parameters mentioned in the formula above are summarized in Table 4.

Table 2. Parameter set for precipitates of AA6xxx in MatCalc

Phase	Nucleation site	Interfacial energy – corr. factor	Volumetric misfit
GP zones	Bulk	0.9	0.01
β''	Bulk	0.85	0.02
β'	Dislocations	0.95	0.00
β	Dislocations	Default value	0.00
Si	Dislocations	Default value	0.05

Table 3. Parameter set for precipitation domain of AA6xxx in MatCalc

Parameter	Value (unit)
Young's modulus	$77.93 \cdot 10^9 - (7.3 \cdot 10^6) \cdot T$ (Pa)
Poisson's ratio	0.33
Dislocation density	$6 \cdot 10^{13}$ (m ⁻²)
Mean diff. distance	Autom. Calc.
Excess Va efficiency	1.0

The volumetric misfit for the GP-zones and the β'' phase are representing the misfit in the surrounding bulk. The latter precipitates are assumed to nucleate at dislocation, where the volumetric misfit between the lattice of the bulk and the phases are negligible. Only for Si, where volumetric misfit is quite large (>20%) [10], a correcting value is set in a reasonable amount of 5% for modeling.

Table 4. Summary of input data used in the strengthening models

Parameter	Value	Comments
r_c	$5 \cdot 10^{-9}$	From [4, 5]
M	3.1	From [4, 5]
β	0.36	From [4, 5]
b (m)	$2.84 \cdot 10^{-10}$	From [4, 5]
G (N/m ²)	$2.7 \cdot 10^{10}$	From [4, 5]
σ_i (MPa)	28	From [7]
k_{Si} (MPa/wt% ^{2/3})	66.3	From [4, 5]
k_{Mg} (MPa/wt% ^{2/3})	29.0	From [4, 5]

Figures 1 and 2 show the simulated yield strength for approaches I and II in comparison to the experimentally measured data.

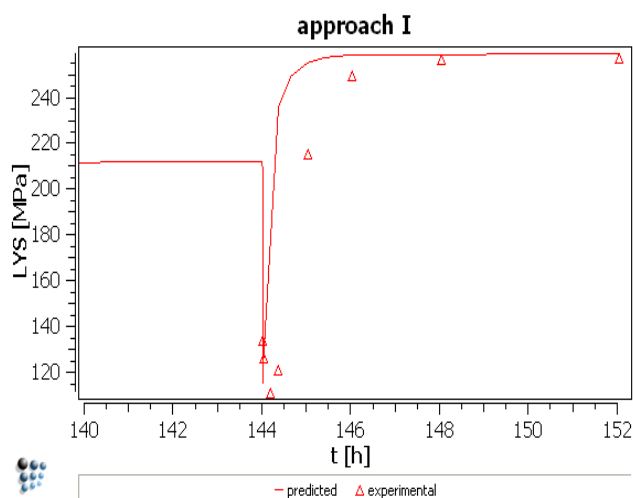


Fig. 1. Approach I – comparison between observed and predicted LYS

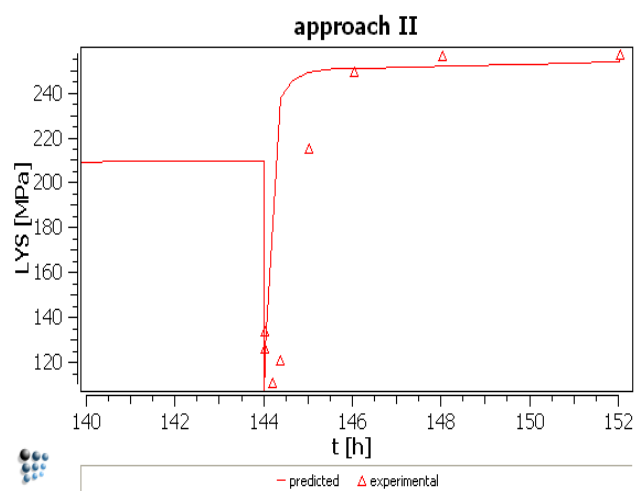


Fig. 2. Approach II – comparison between observed and predicted LYS

5. Summary and conclusion

Both presented models can provide a firm basis for simulation of the evolution of yield strength in Al-Mg-Si alloys. The peak hardness corresponding to the precipitation of beta double prime phase is in accordance with the experimental data. The more generic approach II has the advantage that the overall macroscopic yield strength can be well-understood by all relevant strengthening mechanism and gives information about the influence of each effect. Approach I reaches the same results and is able to give estimations of the yield strength very easily, if the fraction of the phases are available.

In the open literature, the strengthening calculations generally use a mean composition for just one precipitation phase. In the present work, we calculate the effective mechanisms for each phase of the precipitation sequence: GP-zones \rightarrow β'' \rightarrow β' \rightarrow β (Mg_2Si) + Si and, therefore, we are able to analyse the effect of each mechanism for each phase.

Acknowledgement- The authors would like to thank the ARC Leichtmetallkompetenzzentrum Ranshofen GmbH for their cooperation and supports.

References

- [1] <http://www.matcalc.at>, 2010-03-15
- [2] E. Povoden-Karadeniz, P. Warczok, P. Lang, A. Falahati and E. Kozeschnik, (2010) unpublished research
- [3] A. Falahati, E. Povoden-Karadeniz, P. Lang, P. Warczok and E. Kozeschnik (2010) unpublished research
- [4] O. R. Myhr, Ø. Grong and S. J. Andersen: *Acta Materialia* 49 (2001) 65-75
- [5] S. N. Samaras: *Modelling Simul. Mater. Sci. Eng.* 14 (2006) 1271-1292
- [6] I. Holzer, E. Kozeschnik: *Materials Science and Engineering A* (2010) in press
- [7] J. da Costa Teixeira, D. G. Cram, L. Bourgeois, T. J. Bastow, A. J. Hill and C. R. Hutchinson: *Acta Materialia* 56 (2008) 6109-6122
- [8] J. Tani and H. Kido: *Computational Materials Science* 42 (2008) 531-536
- [9] D. N. Seidman, E. A. Marquis and D. C. Dunand: *Acta Materialia* 50 (2002) 4021-4035
- [10] Z. Guo and W. Sha: *Materials Science and Engineering A* 392 (2005) 449-452